



ARTICLE

Hepatic NCoR1 deletion exacerbates alcohol-induced liver injury in mice by promoting CCL2-mediated monocyte-derived macrophage infiltration

Fan Yin¹, Miao-miao Wu¹, Xiao-li Wei², Rui-xue Ren², Meng-hua Liu^{1,3}, Chong-qing Chen^{1,3}, Liu Yang^{1,3}, Rui-qian Xie^{1,3}, Shan-yue Jiang^{1,3}, Xue-fu Wang^{1,3} and Hua Wang^{2,3}

Nuclear receptor corepressor 1 (*NCoR1*) is a corepressor of the epigenetic regulation of gene transcription that has important functions in metabolism and inflammation, but little is known about its role in alcohol-associated liver disease (ALD). In this study, we developed mice with hepatocyte-specific *NCoR1* knockout (*NCoR1*^{Hep-/-}) using the albumin-Cre/LoxP system and investigated the role of *NCoR1* in the pathogenesis of ALD and the underlying mechanisms. The traditional alcohol feeding model and NIAAA model of ALD were both established in wild-type and *NCoR1*^{Hep-/-} mice. We showed that after ALD was established, *NCoR1*^{Hep-/-} mice had worse liver injury but less steatosis than wild-type mice. We demonstrated that hepatocyte-specific loss of *NCoR1* attenuated liver steatosis by promoting fatty acid oxidation by upregulating BMAL1 (a circadian clock component that has been reported to promote peroxisome proliferator activated receptor alpha (*PPARA*)-mediated fatty β -oxidation by upregulating de novo lipid synthesis). On the other hand, hepatocyte-specific loss of *NCoR1* exacerbated alcohol-induced liver inflammation and oxidative stress by recruiting monocyte-derived macrophages via C-C motif chemokine ligand 2 (CCL2). In the mouse hepatocyte line AML12, *NCoR1* knockdown significantly increased ethanol-induced CCL2 release. These results suggest that hepatocyte *NCoR1* plays distinct roles in controlling liver inflammation and steatosis, which provides new insights into the development of treatments for steatohepatitis induced by chronic alcohol consumption.

Keywords: alcohol-associated liver disease; NCoR1; BMAL1; monocyte-derived macrophage; CCL2

Acta Pharmacologica Sinica (2022) 43:2351–2361; <https://doi.org/10.1038/s41401-022-00863-0>

INTRODUCTION

Alcohol-associated liver disease (ALD) is a health problem that is increasingly concerning worldwide [1–3]. The pathogenesis of ALD includes early steatosis and steatohepatitis, and some individuals may eventually progress to fibrosis and liver cirrhosis. Although understanding of the pathological characteristics of ALD has improved, the exact mechanism regulating its pathogenesis is still not very clear. To date, there have been no recognized therapies suitable for preventing or curing this disease. Therefore, further research on the mechanisms that mediate the occurrence and progression of ALD is essential for the development of reasonable therapeutic drugs or technologies for the prevention or clinical treatment of this disease.

Nuclear receptor corepressor 1 (*NCoR1*) acts as a scaffolding protein to mediate several nuclear protein interactions. Interactions between *NCoR1*, nuclear transcription factors, and histone deacetylases (HDACs) have been studied, and these proteins can form a corepressor complex to downregulate target genes [4, 5]. Activation of histone deacetylase 3 (HDAC3) by *NCoR1* plays an important role in the epigenetic regulation of circadian and metabolic physiology [6, 7]. *Bmal1*, which is also known as aryl hydrocarbon receptor

nuclear translocator-like (Arntl), is one of the crucial components of the circadian clock and has been reported to protect against hepatic steatosis by promoting fatty acid oxidation pathways in ALD [8]. It has been reported that the NCoR/HDAC3 complex serves as a corepressor for Rev-erbalpha to regulate the expression of *Bmal1* in human HepG2 hepatocytes [9].

C-C motif chemokine ligand 2 (CCL2), also known as monocyte chemoattractant protein 1 (MCP-1), is closely related to liver inflammation and the recruitment of macrophages to the liver [10]. It has been reported that chronic ethanol administration can upregulate hepatic CCL2 expression and the infiltration and activation of macrophages [11, 12]. Blocking C-C chemokine receptor type 2 and 5 (CCR2/5) signaling pharmacologically prevents and reverses alcohol-induced liver injury in mice [12]. The endocannabinoid anandamide exerts anti-inflammatory effects on vascular smooth muscle cells by inhibiting CCL2 expression by recruiting NCoR1 and histone deacetylase 4 (HDAC4) to the *Ccl2* promoter. In contrast, adipocyte *NCoR1* deletion leads to decreased MCP1 secretion by adipocytes through peroxisome proliferator activated receptor gamma (*PPAR γ*) activation, reducing adipose tissue macrophage levels and decreasing inflammation [13]. However, it is unclear

¹School of Pharmacy, Anhui Medical University, Hefei 230032, China; ²Department of Oncology, the First Affiliated Hospital of Anhui Medical University, Hefei 230022, China and

³Inflammation and Immune Mediated Diseases Laboratory of Anhui Province, Anhui Medical University, Hefei 230032, China

Correspondence: Xue-fu Wang (wangxuefu@ahmu.edu.cn) or Hua Wang (wanghua@ahmu.edu.cn)

These authors contributed equally: Fan Yin, Miao-miao Wu, Xiao-li Wei

Received: 29 September 2021 Accepted: 7 January 2022

Published online: 11 February 2022

whether hepatic *NCoR1* is involved in regulating the release and expression of CCL2 during the pathological process of ALD.

In general, it is believed that steatosis in ALD is positively correlated with liver damage and inflammation. In this study, we revealed that hepatocyte-specific deletion of *NCoR1* increased liver damage and inflammation but unexpectedly ameliorated liver steatosis in ALD models. Mechanistically, our findings suggest that hepatocyte-specific *NCoR1* deficiency reduces alcohol-induced hepatic lipid accumulation by promoting fatty acid oxidation through the upregulation of BMAL1 expression instead of the peroxisome proliferator activated receptor alpha (*PPARα*) protein itself. On the other hand, hepatic deletion of *NCoR1* exacerbated liver inflammation by promoting CCL2 release and monocyte-derived macrophage (MoMF) infiltration. Targeting the NCOR1/CCL2 axis in hepatocytes could be critical for the treatment or prevention of alcohol-induced liver inflammation.

MATERIALS AND METHODS

Animal model

All animal experiments were approved by the Animal Ethics Committee of Anhui Medical University. Male C57BL/6J wild-type (WT) mice were used for the study. Both the traditional model [14] and the NIAAA model [15] of ALD were used as described previously. For the traditional model of ALD, 8-week-old male C57BL/6J mice were fed an ethanol Lieber-DeCarli diet containing 5% (vol/vol) ethanol or an isocaloric control diet for 5 weeks. For the NIAAA model, 8-week-old male C57BL/6J mice were fed either an isocaloric control or ethanol Lieber-DeCarli diet containing 5% (vol/vol) ethanol for 10 days with a single binge (5 g/kg body weight). For conditional *NCoR1* knockout in hepatocytes, B6. Alb-Cre (Strain NO. T003814) and B6. *NCoR1*^{fl/fl} mice (Strain NO. T007978) with a C57BL/6J background were purchased from GemPharmatech Co., Ltd. and were bred and maintained in the Anhui Experimental Animal Center, Anhui Medical University. B6. Alb-Cre mice were crossed with B6. *NCoR1*^{fl/fl} mice to generate *NCoR1*^{fl/fl};Alb-Cre⁻ (*NCoR1*^{fl/fl}) and *NCoR1*^{fl/fl};Alb-Cre⁺ (*NCoR1*^{Hep-/-}) mice. Both male *NCoR1*^{fl/fl};Alb-Cre⁻ and *NCoR1*^{fl/fl};Alb-Cre⁺ mice (8 weeks old) were used in the traditional model and the NIAAA model of ALD for this study. The mice were housed in a controlled temperature (25 ± 1 °C) and humidity (50% ± 5%) environment with a 12-h light/dark cycle and were allowed free access to sterilized food and water.

Protein isolation and Western blotting

Total protein was extracted from liver tissues and hepatocytes using RIPA buffer, and target proteins were examined by Western blotting using specific antibodies as described previously [16]. The anti-NCoR1 antibody (ab3482), anti-BMAL1 antibody (ab235577), and anti-HDAC3 antibody (ab32369) were purchased from Abcam, the anti-PPARα antibody (AF5301) was purchased from Affinity Biosciences, and the anti-β-actin antibody was purchased from Bioss (BS0061R).

Total RNA isolation and quantitative real-time PCR (qPCR)

Total RNA isolation, the generation of cDNA, and qPCR were conducted as previously reported [17]. The primer sequences used are listed in Table 1. The comparative threshold cycle (or 2 Ct) method was used to calculate relative mRNA expression levels.

Biochemical assays

Serum alanine aminotransferase (ALT), aspartate aminotransferase (AST), triglyceride (TG), and total cholesterol (T-CHO) levels were measured with a Mindray automatic biochemical analyzer according to the instructions provided by the commercial assay kits (Shenzhen Mindray Biomedical Electronics Co., Ltd.). Liver TG and T-CHO levels were determined by commercially available assay kits (Nanjing Jiancheng Bioengineering Institute, Nanjing, China).

Table 1. List primers for qPCR.

Gene	Forward primer sequences (5'-3')	Reverse primer sequences (5'-3')
Mouse		
<i>Gapdh</i>	TCAACAGCAACTCCCACTATTCCAC	ACCTGTTGCTGTAGCCGTATTCA
<i>NCoR1</i>	ACAGAGCAAAGTCGTTATCCTTC	GAGCGGTAGTCAGGAACTGC
<i>Srebp1c</i>	AACGTCCTCCAGCTAGAC	CCACTAAGGTGCCTACAGAGC
<i>Fasn</i>	TTGGCCAGAACTCCTGTAG	CTCGTTGTCTGCTGCCT
<i>Srebp2</i>	CCCTATTCCATTGACTCTGAGC	GAGTCCGGTTCATCCTTGAC
<i>Hmgcr</i>	CACAATAACTTCCAGGGGT	GGCCTCCATTAGATCCG
<i>Scd1</i>	TTCTTGCATCACTCTGGTGC	CGGGATTGAATGTTCTTGTCGT
<i>Acc1</i>	GAAGCCACAGTGAAATCTCG	GATGTTTGGCCTTTCACAT
<i>Pparγ</i>	TCGCTGATGCACTGCCTATG	GAGAGGTCCACAGAGCTGATT
<i>Ppara</i>	AACATCGAGTGTGGAATATGTGG	CCGAATAGTTCGCCGAAAGAA
<i>Cpt1a</i>	TCGGTGAGCCTGGCCT	TTGAGTGGTGACCGGACTCG
<i>Fgf21</i>	GTGTCAAAGCCTTAGGTTTCTT	GGTACACATTGTAACCGTCTC
<i>Cyp4a14</i>	TTGCTCACGAGCACACAGAT	TCCTCCATTCTGGCAAACAAGA
<i>Cyp4a10</i>	AGGAGCCAGGAACTGCATTG	GACCTGGTAGGATCTGGCA
<i>Acox1</i>	TAATCTCTCACTCGAAGCCA	AGTTCATGACCCATCTCTGTC
<i>Bmal1</i>	ACAGTCAGATTGAAAAGAGGCG	GCCATCCTTAGCAGGGTGA
<i>Ly6 g</i>	TGCGTTGCTCTGGAGATAGA	CAGAGTAGTGGGGCAGATGG
<i>F4/80</i>	CTGCACCTGTAAACGAGGCTT	GCAGACTGAGTTAGGACCACAA
<i>Tnfa</i>	CAGGCGGTGCCTATGTCTC	GCATACCCCGAAGTCTAGT
<i>IL-6</i>	CTGCAAGAGACTCCATCCAG	AGTGGTATAGACAGGTCTGTTGG
<i>IL-1β</i>	GAAATGCCACCTTTTGACAGTG	TGGATGCTCTCATCAGGACAG
<i>IL-10</i>	CTTACTGACTGGCATGAGGATCA	GCAGCTCTAGGAGCATGTGG
<i>iNOS</i>	GTTCTAGCCCAACAATACAAGA	GTGGACGGTCTGATGTAC
<i>Cyp2e1</i>	ACAGAGACCACCAGACAAC	ATTCATCTGTCTCGGACTGC
<i>Adh1</i>	CCATCGAGGACATAGAAGTCGC	TGGTTTACACAAAGTCAACCC
<i>Adh2</i>	TGGCAGTCCCTTTGTCATT	ACTACCGGAAGAGAGCTTTC
<i>Ccl5</i>	TTTGCTACTCTCCCTCG	CGACTGCAAGATTGGAGCAT
<i>Ccl2</i>	TAAAACCTGGATCGGAACCAA	GCATTAGCTCAGATTTACGGGT
<i>Cxcl1</i>	ACTGCACCCAAACCGAAGTC	TGGGGACACCTTTTAGCATCTT

Histological analysis

Liver tissue samples were fixed in 10% formalin and then processed for embedding and sectioning (5 μm thickness). Liver sections were stained using hematoxylin and eosin (H&E) and Oil Red O according to the standard protocol [18]. Immunohistochemical (IHC) analysis of F4/80 and myeloperoxidase (MPO) was performed to detect inflammation. IHC analysis of 4-hydroxynonenal (4-HNE) was used to detect oxidative stress in liver tissues. For the terminal deoxynucleotidyl transferase dUTP nick end labeling (TUNEL) assay, apoptotic cells were examined using a TUNEL Bright Green Apoptosis Detection Kit (Vazyme Biotech, Nanjing, China) according to the manufacturer's instructions. Slides were scanned by an automatic digital slide scanner (Pannoramic MIDI, 3DHISTECH, Hungary) and analyzed by CaseViewer software. Positively stained areas were quantified, and positive cells were counted using Image-Pro Plus software (×40 magnification) in 3 fields that were randomly selected for each sample.

Isolation and flow cytometric analysis of liver macrophages

Liver macrophages were isolated from NIAAA model mice using a liver perfusion collagenase system as previously reported [19]. Briefly, the liver was perfused with an EGTA perfusion solution for 5 min and IV type collagenase (Sigma) for 10 min, chopped, and filtered using a 70-μm strainer. The nonparenchymal cell fraction was acquired after centrifugation for 5 min at 50 × g. The supernatants were centrifuged for 8 min at 500 × g. Pellets were resuspended in 25% Percoll® (GE Healthcare), transferred to 50% Percoll®, and centrifuged for 20 min at 800 × g. The liver macrophage fraction was isolated from the inner layer between the two different Percoll® gradient layers. Cells were counted and

used for flow cytometry. For flow cytometry, cells were stained with FITC-conjugated anti-mouse CD11b, PE-CY7-conjugated anti-mouse CD45.2, APC-conjugated anti-mouse F4/80, and APC-CY7-conjugated anti-mouse Ly6G antibodies. The data were analyzed by CytExpert software (Beckman Coulter, USA).

Cell culture studies

The AML12 cell line, which is a nontransformed mouse hepatocyte line, was purchased from Yibo Biotechnology Co., Ltd. (Hangzhou, China) and cultured in Dulbecco's modified Eagle's medium/nutrient mixture F12 (DMEM/F12) containing 10% FBS. AML12 cells were treated with ethanol (100 mM) in serum-free DMEM/F12 for 6 h. All cells were maintained in a 37 °C incubator with 5% CO₂.

Gene silencing

AML12 hepatocytes were transfected with mouse siRNAs (*NCoR1*-Mus-598, 5'-GCUUCAAAGGAGGAGUUATT-3' (sense) and 5'-UAACUCCUCCUUUGAAAGCTT-3' (antisense)) for *NCoR1*. As a control, cells were transfected with scramble RNA under the same conditions. These siRNAs were purchased from Gene Pharma Corporation (Shanghai, China). Transfection was performed according to Invitrogen's protocol for Lipofectamine 2000. The transfection results were examined by real-time quantitative PCR (qPCR) after 12 h of siRNA transfection.

ELISA

Organ homogenates, serum, and cell culture supernatants were prepared, and CCL2 protein levels were examined using commercially available ELISA kits (Dakewei, Shanghai, China) according to the instructions provided by the manufacturer.

Statistical analysis

All data are expressed as the mean ± SEM. The sample size was calculated using size power analysis methods (GraphPad Stat-Mate) for a priori determination based on the standard deviations of previous experiments. GraphPad Prism software (version 8.0) was used to calculate statistical significance. Statistical tests were used as described in the figure legends, and statistical significance was indicated as follows: **P* < 0.05; ***P* < 0.01; ****P* < 0.001; ns, not significant.

RESULTS

NCoR1 expression is increased in the liver in ALD mice

First, we constructed two well-established and widely used mouse models of ALD: 1. the traditional Lieber-De Carli diet feeding model (5 weeks of alcohol-containing liquid diet feeding, hereafter referred to as "the traditional model") and 2. the chronic plus binge ethanol feeding model (10 days of an alcohol-containing liquid diet plus one gavage; hereafter referred to as "the NIAAA model"). In the traditional model (Fig. S1a), liver injury was indicated by elevations in ALT and AST levels (Fig. S1b) and H&E staining (Fig. S1c), and marked steatosis was shown by oil red O staining (Fig. S1d) in EtOH-fed mice compared to pair-fed mice. In addition, IHC staining for MPO, a marker of neutrophils, and F4/80, a marker of macrophages, showed that macrophage infiltration increased, whereas neutrophil infiltration was comparable in the livers of EtOH-fed mice compared to that of pair-fed mice (Fig. S1e and f). In the NIAAA model (Fig. S1g), ALT and AST levels were significantly elevated in EtOH-fed mice (Fig. S1h). Histopathological analysis showed that the degree of liver injury was worse (Fig. S1i), and the amount of lipid droplet deposition (Fig. S1j) was significantly higher in EtOH-fed mice than in pair-fed mice. Neutrophil infiltration was markedly increased in EtOH-fed mice, but there was a slight difference in macrophage infiltration (Fig. S1k and l). In summary, we successfully established the traditional model and the NIAAA model of ALD.

Next, to explore the association of hepatic *NCoR1* expression with the pathogenesis of ALD, the expression of *NCoR1* in the livers of ALD mice and pair-fed mice was examined. As shown in Fig. 1a, b, the mRNA level of *NCoR1* in the liver was dramatically increased in WT mice fed an ethanol diet compared to pair-fed WT mice. Similarly, Western blot analysis showed that the protein level of *NCoR1* was higher in the liver in the EtOH-fed groups than in the liver in the control groups (Fig. 1c, d). In short, the abnormally upregulated expression of *NCoR1* in the livers of ethanol-fed mice suggests the potential involvement of *NCoR1* in the pathogenesis of ALD.

Hepatocyte-specific *NCoR1* deficiency sensitizes mice to ethanol-induced liver injury

To explore the role of hepatic *NCoR1* in the pathogenesis of ALD in vivo, we generated hepatocyte-specific *NCoR1* knockout (*NCoR1^{Hep-/-}*) mice (Fig. S2a–d). As controls, floxed *NCoR1* mice

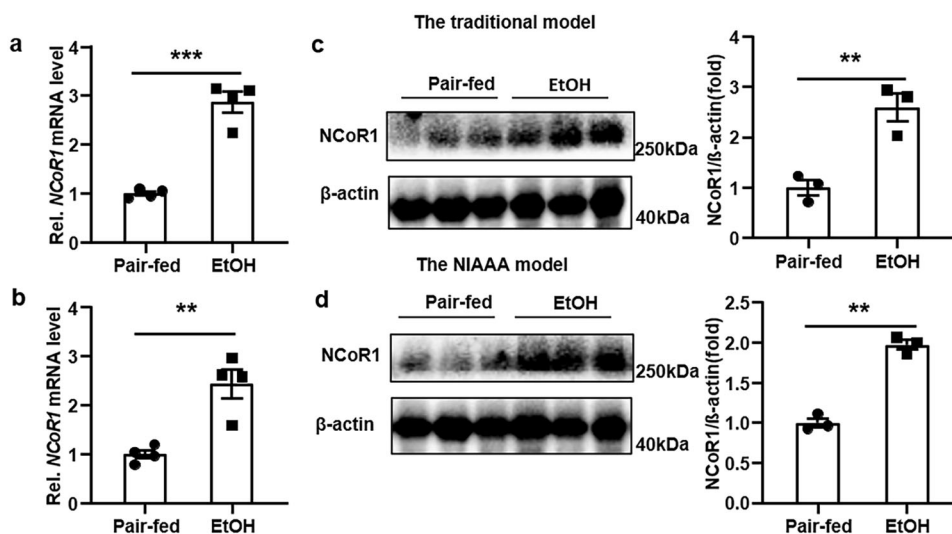


Fig. 1 Hepatic *NCoR1* expression is increased in ALD models. **a** qPCR analysis of hepatic mRNA levels of *NCoR1* in WT mice in the traditional alcohol feeding model (*n* = 4/group). **b** qPCR analysis of hepatic mRNA levels of *NCoR1* in WT mice in the NIAAA model (*n* = 4/group). **c** Western blot analysis of *NCoR1* protein expression in WT mice in the traditional alcohol feeding model (*n* = 3/group). **d** *NCoR1* protein expression in WT mice in the NIAAA model (*n* = 3/group). **P* < 0.05, ***P* < 0.01, ****P* < 0.001 by two-tailed Student's *t* test. *NCoR1*, nuclear receptor corepressor 1.

that did not express Alb-Cre recombinase were used, which are referred to hereafter as *NCoR1^{fl/fl}* mice. Under normal diet feeding, *NCoR1^{Hep-/-}* mice showed normal liver tissue morphology (Fig. S2e) and normal serum ALT levels (Fig. S2f) but slightly upregulated liver TG levels (Fig. S2g), which was consistent with a previous report [20]. Then, we used *NCoR1^{fl/fl}* mice and *NCoR1^{Hep-/-}* mice to generate the traditional model. Body weights, liver weights, and liver-to-body weight ratios for both genotypes under the same diet conditions were not significantly different (Fig. S3a). Intriguingly, ethanol feeding significantly increased serum ALT and AST levels in *NCoR1^{Hep-/-}* mice compared to *NCoR1^{fl/fl}* mice (Fig. 2a). Moreover, H&E staining showed greater liver injury in EtOH-fed *NCoR1^{Hep-/-}* mice than in EtOH-fed *NCoR1^{fl/fl}* mice, which was confirmed by the clear increase in hepatocyte apoptosis, as determined by TUNEL staining (Fig. 2b, c). Next, we further examined this result in the NIAAA model. Body weights, liver weights and liver-to-body weight ratios were comparable between *NCoR1^{Hep-/-}* mice and *NCoR1^{fl/fl}* mice (Fig. S3b). As expected, EtOH-fed *NCoR1^{Hep-/-}* mice showed higher ALT and AST levels (Fig. 2d) and developed more pronounced liver injury and hepatocyte apoptosis (Fig. 2e, f) than EtOH-fed *NCoR1^{fl/fl}* mice. These results suggest that hepatic *NCoR1* deficiency can exacerbate alcohol-induced liver injury.

Hepatocyte-specific deletion of *NCoR1* alleviates alcohol-induced liver lipid accumulation by promoting fatty acid oxidation. Although significant liver damage was observed, fewer fat vacuoles were observed in EtOH-fed *NCoR1^{Hep-/-}* mice, as shown in Fig. 2b, e. Similarly, oil red O staining showed milder lipid droplet accumulation in the livers of *NCoR1^{Hep-/-}* mice than in *NCoR1^{fl/fl}* mice in both the traditional model (Fig. 3a) and the NIAAA model (Fig. 3b). As shown in Fig. 3c, d, serum TG and serum T-CHO levels were comparable between EtOH-fed *NCoR1^{fl/fl}* and EtOH-fed *NCoR1^{Hep-/-}* mice, which might be that because alcohol feeding did not affect serum TG and serum T-CHO concentrations [14]. Furthermore, EtOH-fed *NCoR1^{Hep-/-}* mice showed lower liver TG and liver T-CHO levels than EtOH-fed *NCoR1^{fl/fl}* mice (Fig. 3e, f). Taken together, these data suggest that hepatocyte-specific *NCoR1* deletion reduced alcohol-induced hepatic lipid accumulation.

To understand the mechanisms by which hepatocyte *NCoR1* deletion inhibits ethanol-induced hepatic steatosis. The expression of genes that regulate lipogenesis and β -oxidation was examined. Interestingly, the mRNA levels of both lipogenesis (Fig. 4a, b) and β -oxidation (Fig. 4c, d) genes in the livers of *NCoR1^{Hep-/-}* mice were upregulated compared to those in the livers of *NCoR1^{fl/fl}* mice in the two ALD models. However, hepatic PPAR α protein expression was comparable between *NCoR1^{fl/fl}* mice and *NCoR1^{Hep-/-}* mice (Fig. 4g, h). *Bmal1*, one of the crucial components of the circadian clock, has been reported to promote PPAR α -mediated fatty β -oxidation by upregulating *de novo* lipid synthesis to protect against alcoholic fatty liver disease [8]. Here, we found that, compared to those of *NCoR1^{fl/fl}* mice, both the mRNA level of *Bmal1* (Fig. 4e, f) and the protein level of BMAL1 (Fig. 4g, h) were significantly upregulated in the livers of *NCoR1^{Hep-/-}* mice compared to those of *NCoR1^{fl/fl}* mice after ethanol feeding. In addition, a previous study showed that the NCoR/HDAC3 complex served as a corepressor that regulates the expression of *Bmal1* in HepG2 cells [9]; thus, we examined the protein level of HDAC3. As expected, HDAC3 expression was downregulated in *NCoR1^{Hep-/-}* mice compared to *NCoR1^{fl/fl}* mice in the ALD models (Fig. S4a, b). Collectively, our data suggest that hepatocyte-specific deletion of *NCoR1* could protect mice from ethanol-induced steatosis by upregulating the expression of genes related to fatty acid oxidation via the clock rhythm protein BMAL1.

Hepatocyte-specific *NCoR1* deficiency boosts macrophage infiltration and oxidative stress in the livers of ALD mice. Inflammatory responses are primary contributors to the development and progression of ALD [21]. Worse liver injury but less

liver steatosis was observed in *NCoR1^{Hep-/-}* mice than in *NCoR1^{fl/fl}* mice in the ALD models. We hypothesize that there was more inflammation in EtOH-fed *NCoR1^{Hep-/-}* mice than in control mice. To verify our hypothesis, IHC staining for MPO and F4/80 was performed to test liver inflammation. Interestingly, the number of MPO⁺ neutrophils was comparable in *NCoR1^{fl/fl}* and *NCoR1^{Hep-/-}* mice following ethanol diet feeding (Fig. 5a–c and e). The number of F4/80⁺ macrophages, however, was markedly increased in the livers of EtOH-fed *NCoR1^{Hep-/-}* mice compared to those of EtOH-fed *NCoR1^{fl/fl}* mice (Fig. 5a–c and e). Real-time PCR analysis showed upregulated mRNA levels of F4/80 in the livers of EtOH-fed *NCoR1^{Hep-/-}* mice, but the expression of Ly6G, a marker of neutrophils, was comparable to that of EtOH-fed *NCoR1^{fl/fl}* mice (Fig. 5g, h). Moreover, the expression of the inflammatory factors tumor necrosis factor alpha (*Tnfa*), interleukin 6 (*Il6*), interleukin 1 beta (*Il1 β*), nitric oxide synthase 2, and inducible NOS (*iNOS*) in the livers of *NCoR1^{Hep-/-}* mice were significantly higher than those in *NCoR1^{fl/fl}* mice in the ALD models, and the mRNA level of the anti-inflammatory factor interleukin 10 (*Il10*) was comparable to that in *NCoR1^{fl/fl}* mice (Fig. 5g, h). The infiltration of inflammatory cells can promote the release of reactive oxygen species and reactive nitrogen species, thereby increasing oxidative stress in tissue [22]. IHC analysis of 4-HNE, a marker of oxidative stress, showed that EtOH-fed *NCoR1^{Hep-/-}* mice displayed more positive staining than EtOH-fed *NCoR1^{fl/fl}* mice (Fig. 5a, b, d and f).

These data indicated that hepatocyte-specific *NCoR1* deficiency exacerbated hepatic inflammation and oxidative stress in ALD mice. Next, we examined whether ethanol metabolism contributed to the pathogenesis of ALD in *NCoR1^{Hep-/-}* mice. As shown in Fig. S5a, serum ethanol concentrations were comparable in *NCoR1^{fl/fl}* and *NCoR1^{Hep-/-}* mice at 9 h after ethanol gavage. Real-time PCR analysis showed that hepatic expression of several ethanol metabolizing enzymes, such as cytochrome P450, family 2, subfamily e, polypeptide 1 (*Cyp2e1*), alcohol dehydrogenase 1 (class I) (*Adh1*), alcohol dehydrogenase 4 (class II), and pi polypeptide (*Adh2*), was comparable between *NCoR1^{Hep-/-}* mice and *NCoR1^{fl/fl}* mice in both the pair-fed and EtOH-fed groups (Fig. S5b), indicating that hepatocyte-specific deletion of *NCoR1* did not affect ethanol metabolism.

Hepatocyte-specific *NCoR1* deficiency promotes monocyte-derived macrophage infiltration via CCL2

To further explore the mechanism by which *NCoR1* deletion affects the infiltration of macrophages but not neutrophils in ALD mice, we used flow cytometry to examine the state of resident and infiltrating macrophages in the livers of *NCoR1^{Hep-/-}* and *NCoR1^{fl/fl}* mice in the NIAAA model (Fig. 6a, Fig. S6). Consistent with the IHC results, total liver macrophages (F4/80⁺CD11b⁺) were increased in EtOH-fed *NCoR1^{Hep-/-}* mice compared with EtOH-fed *NCoR1^{fl/fl}* mice (Fig. 6b). However, the infiltration of MoMFs (F4/80^{hi}CD11b^{hi}) was markedly increased in the livers of *NCoR1^{Hep-/-}* mice (Fig. 6c), but the number and proportion of Kupffer cells (KCs, F4/80^{hi}CD11b^{lo}) (Fig. 6d) were comparable in *NCoR1^{fl/fl}* and *NCoR1^{Hep-/-}* mice in the NIAAA model.

To determine the mechanisms by which increased MoMF infiltration occurs in *NCoR1^{Hep-/-}* mice compared to *NCoR1^{fl/fl}* mice in the ALD model, we examined the mRNA levels of the chemokines C-C motif chemokine ligand 5 (*Ccl5*), *Ccl2* (which are implicated in macrophage recruitment to the liver) and (C-X-C motif) ligand 1 (*Cxcl1*) (a key chemokine that promotes neutrophil infiltration) in the livers of *NCoR1^{fl/fl}* and *NCoR1^{Hep-/-}* mice in the traditional model and the NIAAA model. As shown in Fig. 6e and Fig. 6f, the *Ccl2* mRNA level was significantly elevated, whereas *Ccl5* was mildly upregulated and *Cxcl1* was not significantly different in EtOH-fed *NCoR1^{Hep-/-}* mice compared with EtOH-fed *NCoR1^{fl/fl}* mice. Furthermore, ELISA also showed upregulated hepatic CCL2 protein levels (Fig. 6g, h) and serum CCL2 protein

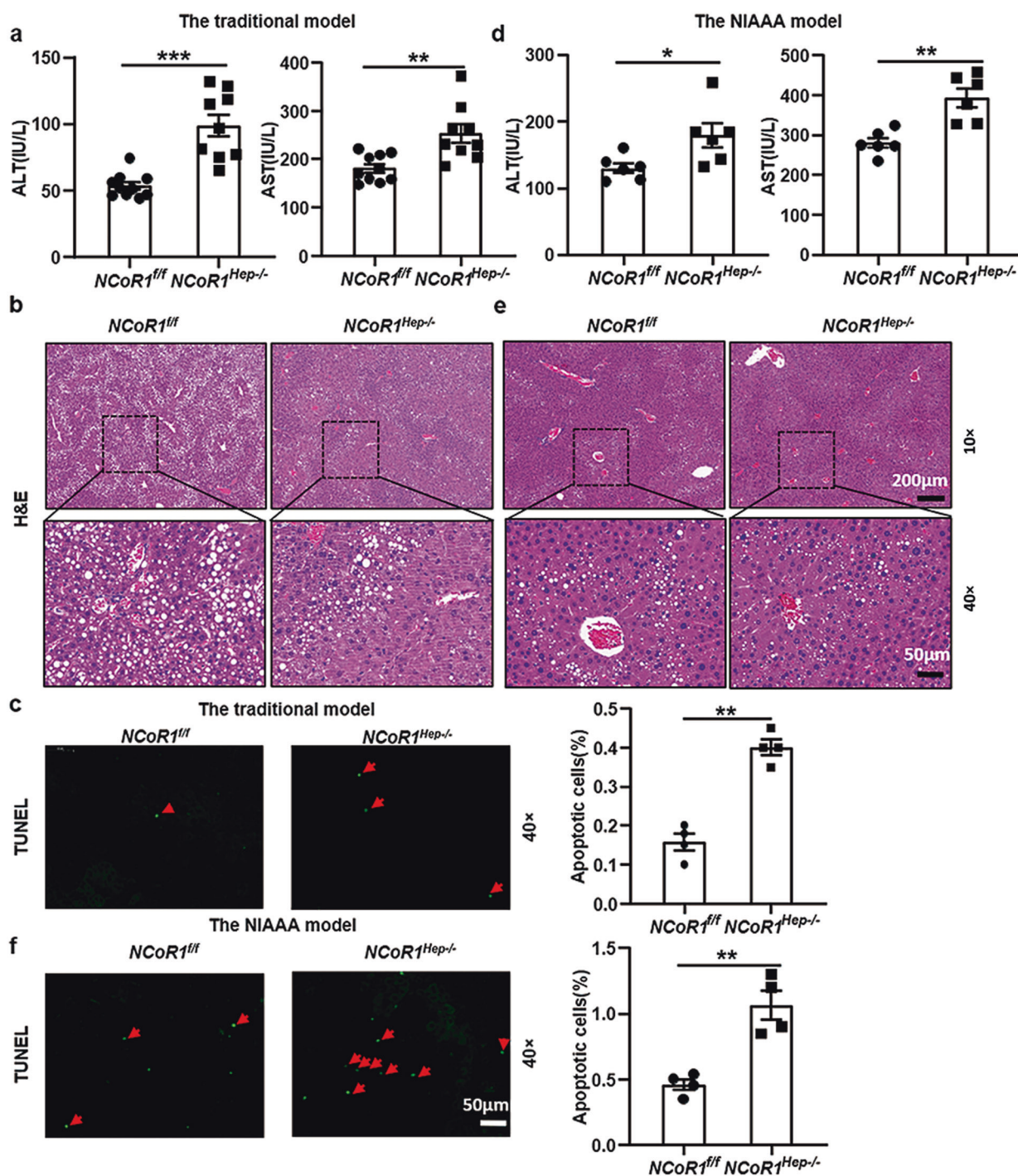


Fig. 2 Hepatic NCoR1 deletion exacerbates alcohol-induced liver injury. *NCoR1^{fl/fl}* mice and *NCoR1^{Hep-/-}* mice were subjected to the traditional alcohol feeding model ($n = 9/\text{group}$) or the NIAAA model of ALD ($n = 6/\text{group}$). **a** Serum ALT and AST levels of EtOH-fed *NCoR1^{fl/fl}* mice and EtOH-fed *NCoR1^{Hep-/-}* mice in the traditional alcohol feeding model ($n = 9/\text{group}$). **b** Representative H&E staining of liver tissue from EtOH-fed *NCoR1^{fl/fl}* mice and EtOH-fed *NCoR1^{Hep-/-}* mice in the traditional alcohol feeding model ($n = 6/\text{group}$). **c** TUNEL staining and quantification of EtOH-fed *NCoR1^{fl/fl}* mice and EtOH-fed *NCoR1^{Hep-/-}* mice in the traditional alcohol feeding model ($n = 4/\text{group}$). **d** Serum ALT and AST levels of EtOH-fed *NCoR1^{fl/fl}* mice and EtOH-fed *NCoR1^{Hep-/-}* mice in the NIAAA model ($n = 6/\text{group}$). **e** Representative H&E staining of the liver tissue of EtOH-fed *NCoR1^{fl/fl}* mice and EtOH-fed *NCoR1^{Hep-/-}* mice in the NIAAA model ($n = 6/\text{group}$). **f** TUNEL staining and quantification of EtOH-fed *NCoR1^{fl/fl}* mice and EtOH-fed *NCoR1^{Hep-/-}* mice in the NIAAA model ($n = 4/\text{group}$). * $P < 0.05$, ** $P < 0.01$, *** $P < 0.001$ by two-tailed Student's t test. 10 \times , Scale bar = 200 μm ; 40 \times , Scale bar = 50 μm . ALT, alanine aminotransferase; AST, aspartate aminotransferase; H&E, hematoxylin and eosin; TUNEL, terminal deoxynucleotidyl transferase dUTP nick end labeling.

levels (Fig. 6i, j) in EtOH-fed *NCoR1^{Hep-/-}* mice compared to EtOH-fed *NCoR1^{fl/fl}* mice. To further determine the regulatory effect of NCoR1 on CCL2, we used the mouse hepatocyte line AML12 and treated the cells with EtOH (100 mM) for 6 h. Interestingly,

EtOH-mediated upregulation of CCL2 production was markedly enhanced in the *NCoR1* siRNA group (Fig. S7a, b). In summary, hepatic *NCoR1* deletion promoted MoMF infiltration via CCL2 in the livers of ALD mice.

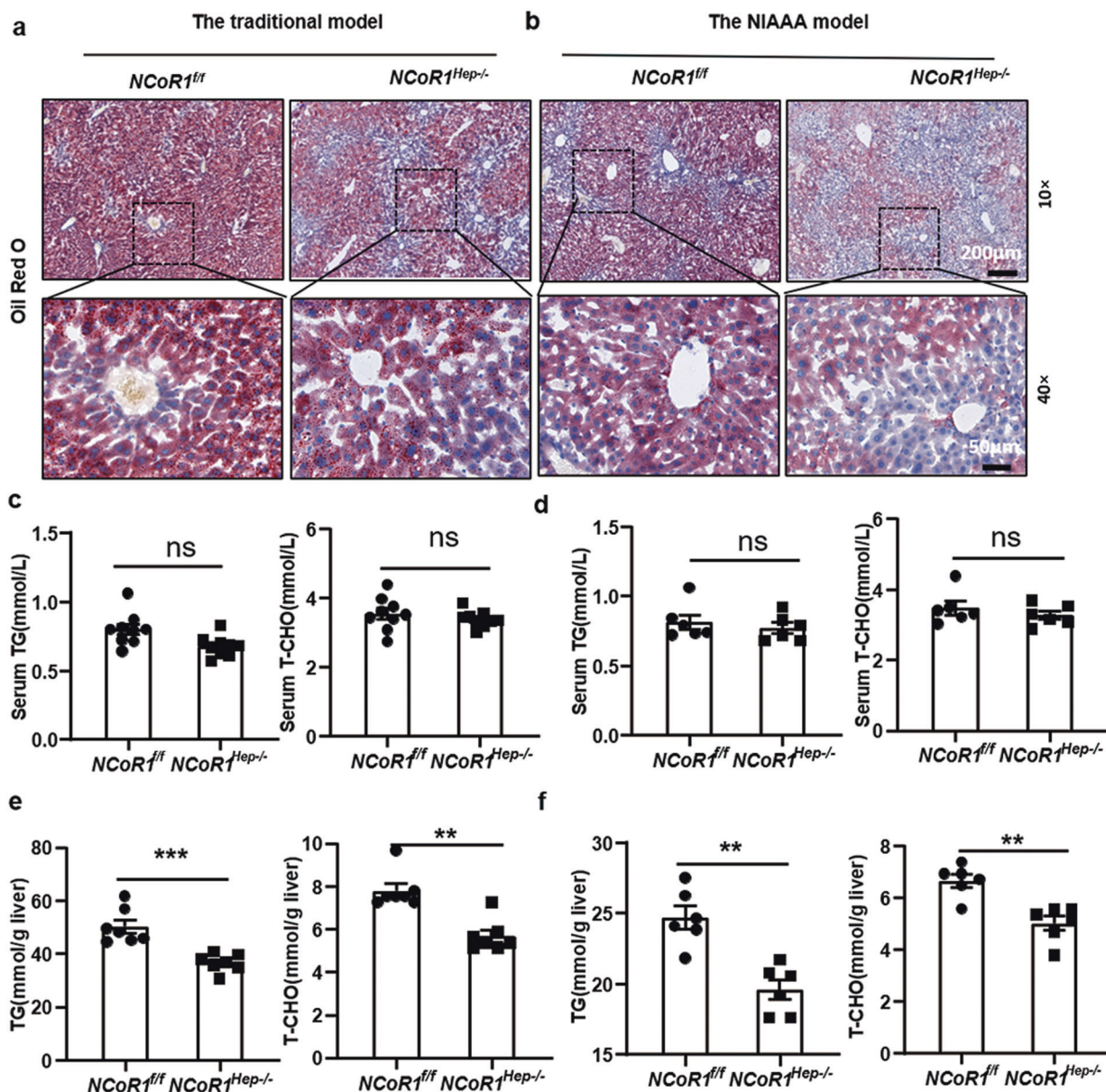


Fig. 3 Hepatic NCoR1 deletion reduces alcohol-induced liver lipid accumulation. **a, b** Oil Red O staining of liver tissues from EtOH-fed *NCoR1^{fl/fl}* mice and EtOH-fed *NCoR1^{Hep-/-}* mice in **a** the traditional alcohol feeding model ($n = 6$ /group) and **b** the NIAAA model ($n = 6$ /group). **c, d** Serum TG and T-CHO levels in EtOH-fed *NCoR1^{fl/fl}* mice and EtOH-fed *NCoR1^{Hep-/-}* mice in **(c)** the traditional alcohol feeding model ($n = 9$ /group) and **d** the NIAAA model ($n = 6$ /group). **e, f** Liver TG and T-CHO levels in EtOH-fed *NCoR1^{fl/fl}* mice and EtOH-fed *NCoR1^{Hep-/-}* mice in **e** the traditional alcohol feeding model ($n = 9$ /group) and **f** in the NIAAA model ($n = 6$ /group). * $P < 0.05$, ** $P < 0.01$, *** $P < 0.001$, by two-tailed Student's *t* test. 10x, Scale bar = 200 μm; 40x, Scale bar = 50 μm. TG, triglyceride; T-CHO, total cholesterol.

DISCUSSION

In this study, we provide initial evidence that hepatocyte *NCoR1* is involved in the pathogenesis of ALD. By using two ALD models, we showed that the expression of hepatic *NCoR1* was upregulated in ALD mice. Further research demonstrated that hepatocyte-specific *NCoR1* knockout exacerbated alcohol-induced liver injury and inflammation by increasing CCL2 release but alleviated alcohol-induced hepatic steatosis by upregulating BMAL1 expression. These findings have been integrated into a model that depicts the potential roles of hepatic *NCoR1* in ALD (Fig. 7).

Abnormal upregulation of *NCoR1* expression in the livers of the ALD models suggests the possible role of *NCoR1* during the occurrence and development of ALD. However, the exact mechanism by which *NCoR1* is increased is unclear and needs to be determined in the future. Since hepatocytes account for 70%

of the total number of cells in the liver [23], we generated *NCoR1^{Hep-/-}* mice.

Steatosis is considered to be a major feature of ALD. Previous studies have reported that *NCoR1^{Hep-/-}* mice show characteristics of steatosis [20]. Moreover, hepatic *NCoR1* disruption enhanced hepatocyte proliferation after partial hepatectomy and attenuated the formation of neoplastic lesions by promoting de novo fatty acid synthesis [20]. Surprisingly, EtOH-fed *NCoR1^{Hep-/-}* mice showed milder hepatic lipid accumulation than control mice. In the ALD models, hepatocyte-specific knockout of *NCoR1* upregulated the expression of both lipogenesis and β -oxidation genes in the livers of ALD mice. However, PPAR α protein expression was comparable between EtOH-fed *NCoR1^{Hep-/-}* mice and control mice. Previous studies have shown that Bmal1 is a direct target of the NCoR/HDAC complex in hepatocytes [24]. Hepatic BMAL1

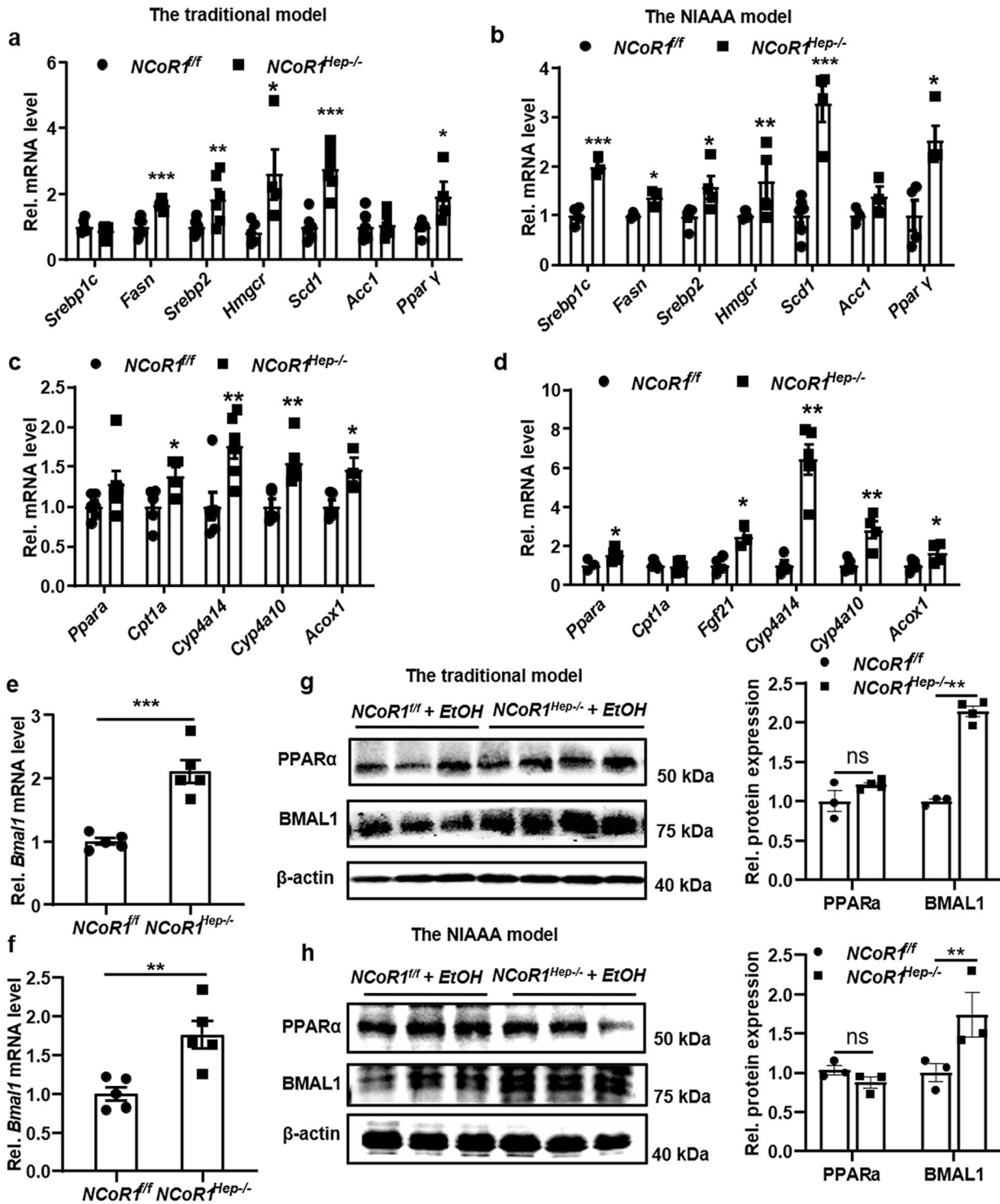


Fig. 4 Hepatic NCoR1 deletion promotes fatty acid oxidation in the ALD models by upregulating BMAL1 expression. **a, b** qPCR analysis of hepatic mRNA levels of lipogenic genes in EtOH-fed *NCoR1^{fl/fl}* mice and EtOH-fed *NCoR1^{Hep-/-}* mice in **a** the traditional alcohol feeding model ($n = 4-6/\text{group}$) and **b** the NIAAA model ($n = 4-6/\text{group}$). **c, d** qPCR analysis of hepatic mRNA levels of PPARα target genes in EtOH-fed *NCoR1^{fl/fl}* mice and EtOH-fed *NCoR1^{Hep-/-}* mice in **c** the traditional alcohol feeding model ($n = 4-6/\text{group}$) and **d** the NIAAA model ($n = 4-6/\text{group}$). **e, f** qPCR analysis of hepatic mRNA levels of *Bmal1* in EtOH-fed *NCoR1^{fl/fl}* mice and EtOH-fed *NCoR1^{Hep-/-}* mice in **e** the traditional alcohol feeding model ($n = 4-6/\text{group}$) and **f** the NIAAA model ($n = 4-6/\text{group}$). **g, h** Western blot analysis of hepatic protein levels of PPARα and BMAL1 in EtOH-fed *NCoR1^{fl/fl}* mice and EtOH-fed *NCoR1^{Hep-/-}* mice in **(g)** the traditional alcohol feeding model ($n = 3-4/\text{group}$) and **(h)** the NIAAA model ($n = 3/\text{group}$). * $P < 0.05$, ** $P < 0.01$, *** $P < 0.001$, by two-tailed Student's *t* test. *Srebp1c*, sterol regulatory transcription factor 1; *Fasn*, fatty acid synthase; *Srebp2*, sterol regulatory element binding protein 2; *Hmgcr*, 3-hydroxy-3-methylglutaryl-Coenzyme A reductase; *Scd1*, stearoyl-Coenzyme A desaturase 1; *Acc1*, acetyl-Coenzyme A carboxylase alpha; *Pparγ*, peroxisome proliferator activated receptor gamma; *Ppara*, peroxisome proliferator activated receptor alpha; *Cpt1a*, carnitine palmitoyltransferase 1a; *Cyp4a14*, cytochrome P450, family 4, subfamily a, polypeptide 14; *Cyp4a10*, cytochrome P450, family 4, subfamily a, polypeptide 10; *Acox1*, acyl-Coenzyme A oxidase 1, palmitoyl; *Fgf21*, fibroblast growth factor 21.

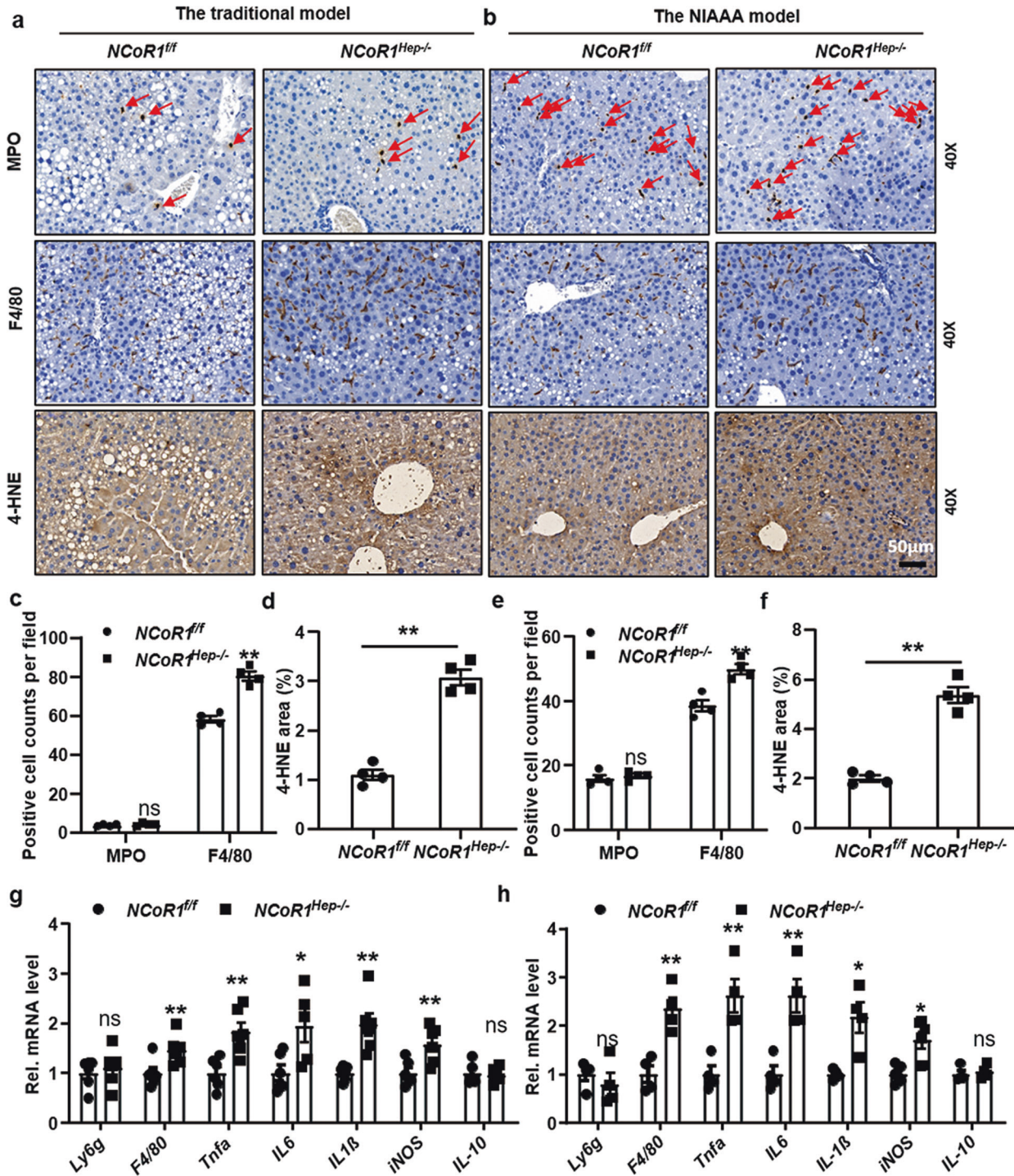


Fig. 5 Hepatic NCoR1 deletion exacerbates liver inflammation and oxidative stress in ALD models. **a–f** IHC staining and quantification of MPO, F4/80 and 4-HNE in the liver tissues of EtOH-fed *NCoR1^{fl/fl}* mice and EtOH-fed *NCoR1^{Hep-/-}* mice in **a, c, d** the traditional alcohol feeding model ($n = 4$ /group) and **b, e, f** the NIAAA model ($n = 4$ /group). **g, h** qPCR analysis of hepatic mRNA levels of inflammation-related genes in EtOH-fed *NCoR1^{fl/fl}* mice and EtOH-fed *NCoR1^{Hep-/-}* mice in **g** the traditional alcohol feeding model ($n = 4–6$ /group) and **h** the NIAAA model ($n = 4–6$ /group). * $P < 0.05$, ** $P < 0.01$, by two-tailed Student's t test. 40x, Scale bar = 50 μm. MPO, myeloperoxidase; 4-HNE, 4-hydroxynonenal; *Tnfa*, tumor necrosis factor α ; *IL6*, interleukin 6; *IL1 β* , interleukin 1 beta; *iNOS*, nitric oxide synthase 2, inducible; *IL10*, interleukin 10.

protects against chronic high-fat diet (HFD)-induced liver steatosis [25]. Importantly, Zhang D et al. reported that hepatic Bmal1 protected mice from alcohol-induced liver steatosis by promoting PPAR α -mediated fatty oxidation by upregulating the expression of de novo lipogenesis genes [8]. In the present study, both the mRNA level of *Bmal1* and the protein level of BMAL1

were upregulated in the livers of *NCoR1^{Hep-/-}* mice compared with *NCoR1^{fl/fl}* mice following ethanol feeding. This finding appropriately explains why hepatic *NCoR1* deletion reduced alcohol-induced liver steatosis.

In addition to steatosis, inflammation is another important key element during the pathogenesis of ALD. To date, several studies

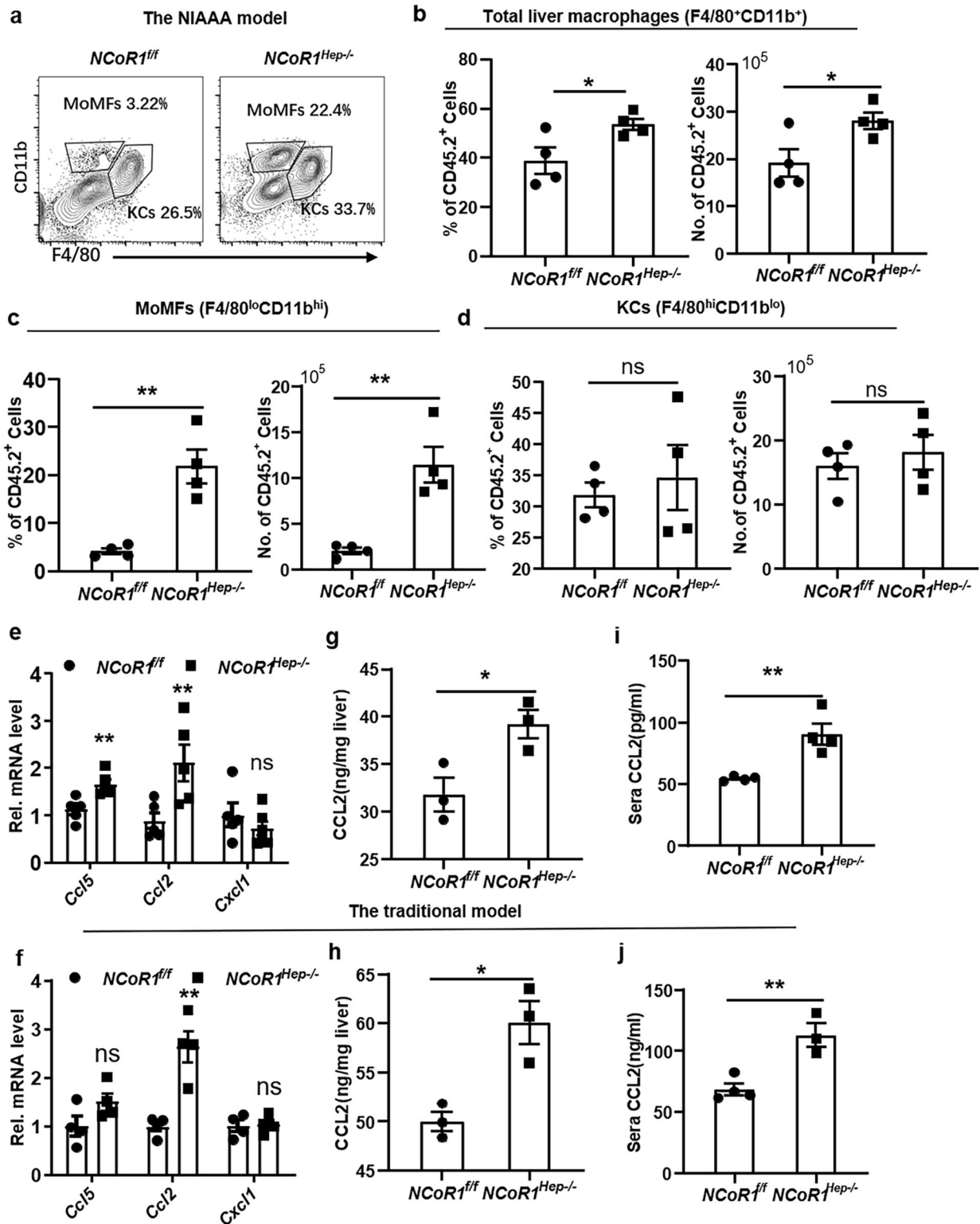


Fig. 6 Hepatic NCoR1 deficiency increases CCL2 expression and MoMF infiltration in the livers of ALD mice. **a–d** Frequency of the proportions and numbers of **b** total liver macrophages, **c** MoMFs and **d** KCs among CD45.2⁺ cells from the livers of EtOH-fed *NCoR1^{fl/fl}* mice and EtOH-fed *NCoR1^{Hep-/-}* mice in the NIAAA model ($n = 4$ /group). **e, f** qPCR analysis of hepatic mRNA levels of chemokines in EtOH-fed *NCoR1^{fl/fl}* mice and EtOH-fed *NCoR1^{Hep-/-}* mice in **e** the NIAAA model ($n = 4–6$ /group) and **f** the traditional alcohol feeding model ($n = 4–6$ /group). **g, h** Protein levels of CCL2 in the livers of EtOH-fed *NCoR1^{fl/fl}* mice and EtOH-fed *NCoR1^{Hep-/-}* mice in **g** the NIAAA model ($n = 3$ /group) and **h** the traditional alcohol feeding model ($n = 3$ /group). **i–j** Protein levels of CCL2 in the sera of EtOH-fed *NCoR1^{fl/fl}* mice and EtOH-fed *NCoR1^{Hep-/-}* mice in **i** the NIAAA model ($n = 4$ /group) and **j** the traditional alcohol feeding model ($n = 3–4$ /group). * $P < 0.05$, ** $P < 0.01$, by two-tailed Student's *t* test. MoMFs, monocyte-derived macrophages; KCs, Kupffer cells; *Ccl5*, C-C motif chemokine ligand 5; *Ccl2*, C-C motif chemokine ligand 2; *Cxcl1*, chemokine (C-X-C motif) ligand 1.

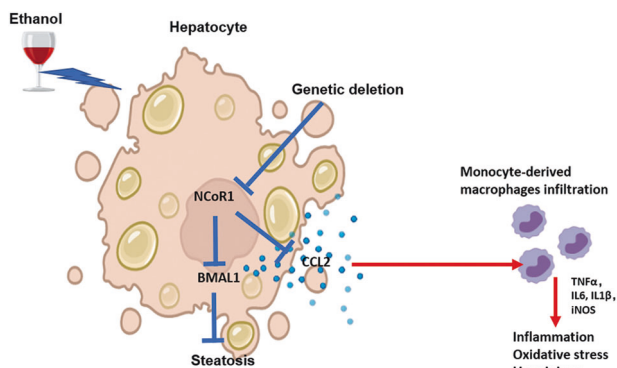


Fig. 7 The potential dichotomic role of hepatic NCoR1 in an ALD model. Briefly, under chronic alcohol consumption conditions, hepatic NCoR1 deletion reduces lipid accumulation by promoting fatty acid β oxidation, which is attributed to upregulation of the BMAL1/lipogenesis axis. In contrast, hepatic NCoR1 deletion exacerbates alcohol-induced liver injury and inflammation by promoting CCL2-mediated MoMF infiltration.

have reported that *NCoR1* in macrophages and other cells regulates inflammation [26–28], but there has been no research on hepatocytes. In this study, we first revealed the mechanism underlying hepatocyte *NCoR1*-regulated liver inflammation in ALD mice. Macrophages and neutrophils play important roles in alcoholic steatohepatitis (ASH). In chronic ASH, on the one hand, alcohol activates hepatic macrophages to produce proinflammatory cytokines; on the other hand, stressed hepatocytes and activated KCs produce chemokines, such as CCL2, which increase the infiltration of MoMFs, thereby promoting the progression of ASH [21, 29]. Conversely, previous studies revealed that binge alcohol feeding significantly increased neutrophil infiltration in the liver and circulation in chronic ethanol-fed mice [30] and in human alcoholic patients [31]. In the current study, markedly elevated infiltration of hepatic neutrophils was observed after chronic ethanol feeding plus one binge; interestingly, there was no apparent difference between *NCoR1*^{fl/fl} mice and *NCoR1*^{Hep-/-} mice. However, we found that hepatocyte-specific *NCoR1* deletion markedly elevated macrophage infiltration after 5 weeks of ethanol feeding and chronic plus binge feeding. CCL2, a key chemokine that promotes macrophage infiltration, has been reported to be markedly elevated and to play an important role in the liver in ASH patients [12, 32]. Fascinatingly, we found that hepatic CCL2 expression was significantly elevated in EtOH-fed *NCoR1*^{Hep-/-} mice compared to EtOH-fed *NCoR1*^{fl/fl} mice, indicating that hepatocyte *NCoR1* plays an important role in regulating CCL2 expression, which was verified in murine AML12 cells in vitro. In summary, our study reveals for the first time that hepatocyte *NCoR1* is involved in macrophage-mediated hepatic inflammation induced by chronic alcohol consumption by regulating the expression and release of hepatic CCL2. However, the exact mechanism is still unclear. We hypothesize that the molecular mechanism by which hepatocyte *NCoR1* regulates *Ccl2* expression may be that alcohol promotes *NCoR1*/HDAC complex binding to the promoter region of *Ccl2*. Another possible reason is that *NCoR1* inhibits the activation of the NF- κ B pathway, which has been reported to be crucial for *Ccl2* gene expression [33]. Further research is warranted to clarify the precise contribution of this pathway to the beneficial effect of regulating CCL2 expression in the prevention and treatment of alcoholic steatohepatitis.

In general, lipid accumulation is positively correlated with inflammation and liver damage in metabolic-related liver diseases. However, in our ethanol-fed *NCoR1*^{Hep-/-} model mice had less steatosis than control mice but a higher degree of liver inflammation and injury, suggesting that inflammation was not

entirely dependent on lipid accumulation. This conclusion was also supported by several other studies. For example, Horiguchi N et al. reported that hepatocyte *STAT3* promoted liver inflammation but ameliorated alcoholic fatty liver [34]. Zhang D et al. reported that hepatic *Bmal1* deletion significantly exacerbated alcohol-induced steatosis but did not affect liver inflammation [8]. In addition, hepatocyte *Shp1* deletion promoted hepatic lipid accumulation but reduced hepatic inflammation and hepatocellular damage in HFD-induced nonalcoholic fatty liver disease (NAFLD) [35]. These findings suggest that lipid accumulation and inflammation induced by alcohol consumption play a synergistic but independent role in promoting liver damage.

In conclusion, we demonstrate a novel mechanism by which hepatocyte *NCoR1* regulates liver inflammation and steatosis in ALD. The *NCoR1*-CCL2 axis identified in the current study yields new insights into the development of potential treatments for monocyte-mediated steatohepatitis induced by chronic alcohol consumption.

ACKNOWLEDGEMENTS

This study was supported by the National Natural Science Foundation of China (81770588/H0315).

AUTHOR CONTRIBUTIONS

FY, MMW, XLW designed and conducted the experiments; RXR, MHL, CQC, LY, RQX, SYJ conducted the experiments; and FY, MMW, XLW, RXR analyzed and interpreted the data. FY, MMW, XLW, RXR, XFW, HW wrote the manuscript. XFW and HW conceptualized and supervised the study.

ADDITIONAL INFORMATION

Supplementary information The online version contains supplementary material available at <https://doi.org/10.1038/s41401-022-00863-0>.

Competing interests: The authors declare no competing interests.

REFERENCES

- Asrani S, Devarbhavi H, Eaton J, Kamath P. Burden of liver diseases in the world. *J Hepatol*. 2019;70:151–71.
- Im G, Cameron AJ, Lucey M. Liver transplantation for alcoholic hepatitis. *J Hepatol*. 2019;70:328–34.
- Asrani S, Mellinger J, Arab J, Shah V. Reducing the global burden of alcohol-associated liver disease: a blueprint for action. *Hepatology*. 2021;73:2039–50.
- Hogg S, Motorna O, Cluse L, Johanson T, Coughlan H, Raviram R, et al. Targeting histone acetylation dynamics and oncogenic transcription by catalytic P300/CBP inhibition. *Mol Cell*. 2021;81:2183–200. e13.
- Chen Z, Huo D, Li L, Liu Z, Li Z, Xu S, et al. Nuclear DEK preserves hematopoietic stem cells potential via *NCoR1*/HDAC3-Akt1/2-mTOR axis. *J Exp Med*. 2021;218:e20201974.
- Kim Y, Marhon S, Zhang Y, Steger D, Won K, Lazar MJMe. Rev-erba dynamically modulates chromatin looping to control circadian gene transcription. *Science*. 2018;359:1274–7.
- Jordan S, Kriebbs A, Vaughan M, Duglan D, Fan W, Henriksson E, et al. *CRY1/2* selectively repress *PPAR δ* and limit exercise capacity. *Cell Metab*. 2017;26:243–55. e6.
- Zhang D, Tong X, Nelson BB, Jin E, Sit J, Charney N, et al. The hepatic *BMAL1*/AKT/lipogenesis axis protects against alcoholic liver disease in mice via promoting *PPAR* pathway. *Hepatology*. 2018;68:883–96.
- Yin L, Lazar M. The orphan nuclear receptor Rev-erbalph recruits the *N-CoR*/histone deacetylase 3 corepressor to regulate the circadian *Bmal1* gene. *Mol Endocrinol*. 2005;19:1452–9.
- Cao S, Liu M, Sehrawat T, Shah V. Regulation and functional roles of chemokines in liver diseases. *Nat Rev Gastroenterol*. 2021;18:630–47.
- Mandrekar P, Ambade A, Lim A, Szabo G, Catalano D. An essential role for monocyte chemoattractant protein-1 in alcoholic liver injury: regulation of proinflammatory cytokines and hepatic steatosis in mice. *Hepatology*. 2011;54:2185–97.
- Ambade A, Lowe P, Kodys K, Catalano D, Gyongyosi B, Cho Y, et al. Pharmacological inhibition of CCR2/5 signaling prevents and reverses alcohol-induced liver damage, steatosis, and inflammation in mice. *Hepatology*. 2019;69:1105–21.

13. Li P, Fan W, Xu J, Lu M, Yamamoto H, Auwerx J, et al. Adipocyte NCoR knockout decreases PPARgamma phosphorylation and enhances PPARgamma activity and insulin sensitivity. *Cell*. 2011;147:815–26.
14. Song Q, Chen Y, Wang J, Hao L, Huang C, Griffiths A, et al. ER stress-induced upregulation of NNMT contributes to alcohol-related fatty liver development. *J Hepatol*. 2020;73:783–93.
15. Bertola A, Mathews S, Ki SH, Wang H, Gao B. Mouse model of chronic and binge ethanol feeding (the NIAAA model). *Nat Protoc*. 2013;8:627–37.
16. Zeng X, Li X, Xu C, Jiang F, Mo Y, Fan X, et al. Schisandra sphenanthera extract (Wuzhi Tablet) protects against chronic-binge and acute alcohol-induced liver injury by regulating the NRF2-ARE pathway in mice. *Acta Pharm Sin*. 2017;7:583–92. B
17. Ramirez T, Li YM, Yin S, Xu MJ, Feng D, Zhou Z, et al. Aging aggravates alcoholic liver injury and fibrosis in mice by downregulating sirtuin 1 expression. *J Hepatol*. 2017;66:601–9.
18. Luther J, Khan S, Gala MK, Kedrin D, Sridharan G, Goodman RP, et al. Hepatic gap junctions amplify alcohol liver injury by propagating cGAS-mediated IRF3 activation. *Proc Natl Acad Sci USA*. 2020;117:11667–73.
19. Zhang X, Goncalves R, Mosser D. The isolation and characterization of murine macrophages. *Curr Protoc Immunol*. 2008:Unit 14.1.
20. Ou-Yang Q, Lin XM, Zhu YJ, Zheng B, Li L, Yang YC, et al. Distinct role of nuclear receptor corepressor 1 regulated de novo fatty acids synthesis in liver regeneration and hepatocarcinogenesis in mice. *Hepatology*. 2018;67:1071–87.
21. Gao B, Ahmad MF, Nagy LE, Tsukamoto H. Inflammatory pathways in alcoholic steatohepatitis. *J Hepatol*. 2019;70:249–59.
22. Ge X, Leung T, Arriazu E, Lu Y, Urtasun R, Christensen B, et al. Osteopontin binding to lipopolysaccharide lowers tumor necrosis factor- α and prevents early alcohol-induced liver injury in mice. *Hepatology*. 2014;59:1600–16.
23. Gao B, Jeong WI, Tian Z. Liver: An organ with predominant innate immunity. *Hepatology*. 2008;47:729–36.
24. Yin L, Lazar MA. The orphan nuclear receptor Rev-erb α recruits the N-CoR/histone deacetylase 3 corepressor to regulate the circadian Bmal1 gene. *Mol Endocrinol*. 2005;19:1452–9.
25. Jacobi D, Liu S, Burkewitz K, Kory N, Knudsen N, Alexander R, et al. Hepatic Bmal1 regulates rhythmic mitochondrial dynamics and promotes metabolic fitness. *Cell Metab*. 2015;22:709–20.
26. Oppi S, Nusser-Stein S, Blyszczuk P, Wang X, Jomard A, Marzolla V, et al. Macrophage NCOR1 protects from atherosclerosis by repressing a pro-atherogenic PPARgamma signature. *Eur Heart J*. 2020;41:995–1005.
27. Kubota T, Inoue M, Kubota N, Takamoto I, Mineyama T, Iwayama K, et al. Downregulation of macrophage Irs2 by hyperinsulinemia impairs IL-4-induced M2a-subtype macrophage activation in obesity. *Nat Commun*. 2018;9:4863.
28. Glass CK, Saijo K. Nuclear receptor transrepression pathways that regulate inflammation in macrophages and T cells. *Nat Rev Immunol*. 2010;10:365–76.
29. Wang M, You Q, Lor K, Chen F, Gao B, Ju C. Chronic alcohol ingestion modulates hepatic macrophage populations and functions in mice. *J Leukoc Biol*. 2014;96:657–65.
30. Bertola A, Park O, Gao B. Chronic plus binge ethanol feeding synergistically induces neutrophil infiltration and liver injury in mice: a critical role for E-selectin. *Hepatology*. 2013;58:1814–23.
31. Li M, He Y, Zhou Z, Ramirez T, Gao Y, Gao Y, et al. MicroRNA-223 ameliorates alcoholic liver injury by inhibiting the IL-6-p47-oxidative stress pathway in neutrophils. *Gut*. 2017;66:705–15.
32. Marin V, Poulsen K, Odena G, McMullen MR, Altamirano J, Sancho-Bru P, et al. Hepatocyte-derived macrophage migration inhibitory factor mediates alcohol-induced liver injury in mice and patients. *J Hepatol*. 2017;67:1018–25.
33. Wolter S, Doerrie A, Weber A, Schneider H, Hoffmann E, von der Ohe J, et al. c-Jun controls histone modifications, NF-kappaB recruitment, and RNA polymerase II function to activate the ccl2 gene. *Mol Cell Biol*. 2008;28:4407–23.
34. Horiguchi N, Wang L, Mukhopadhyay P, Park O, Jeong WI, Lafdil F, et al. Cell type-dependent pro- and anti-inflammatory role of signal transducer and activator of transcription 3 in alcoholic liver injury. *Gastroenterology*. 2008;134:1148–58.
35. Xu E, Forest M, Schwab M, Avramoglu R, St-Amand E, Caron A, et al. Hepatocyte-specific Ptpn6 deletion promotes hepatic lipid accretion, but reduces NAFLD in diet-induced obesity: potential role of PPAR γ . *Hepatology*. 2014;59:1803–15.